Model-independent analysis on the regular behavior of α preformation probability in heavy nuclei

Shulin Tang and Yibin Qian*
Department of Applied Physics and MIIT Key Laboratory of Semiconductor Microstructure and Quantum Sensing, Nanjing University of Science and Technology, Nanjing 210094, China

Zhongzhou Ren
School of Physics Science and Engineering, Tongji University, Shanghai 200092, China

(Received 14 September 2023; accepted 9 November 2023; published 5 December 2023)

The formation process of the α cluster at the surface of nuclei is believed to unravel the structural properties of heavy nuclei, while the fully microscopic understanding of the formation probability is still extremely difficult. In this study, the α decay width is obtained within the cluster model plus the identical α-core interaction potential for our previous α-cluster structure investigation. Given that the α decay half-life is determined by the decay width (penetration probability) and the α preformation probability (P_α), the relative-varying trend of P_α can be then systematically analyzed via the comparison of the ratio of experimental α decay half-lives in isotopic chains with that of calculated decay widths to avoid exploring the model-dependent values of preformation probabilities. The ratio of extracted P_α values, for neighboring α emitters, is further presented to clearly reveal the smooth pattern of the formation probabilities of the α cluster off the shell closure. As a comparative study, the ratio of the P_α value from the cluster formation model is listed in the valence nucleon scheme as well, showing a similar pattern to the present results.

DOI: 10.1103/PhysRevC.108.064303

I. INTRODUCTION

α decay, as one crucial decay channel of unstable nuclei, has received extensive attention since the early stages of nuclear physics especially due to its key role played in the identification of newly synthesized heaviest nuclides [1–4]. On the other hand, the spectra of α decay provide us a unique platform to explore the structural properties of exotic nuclei [5–10], such as the robustness of the $N = 126$ neutron shell [11], the proton-neutron pairing correlation [12–15], and the odd-even staggering phenomenon [16–20]. Theoretically, the α decay is usually treated as a two-step process, namely, the formation of the α cluster and its subsequential penetration through the Coulomb barrier. The latter procedure was independently interpreted by Gamow [21] and Gurney and Condon [22] as the quantum tunneling phenomenon, which is the first successful application of quantum mechanics into the nuclear physics field. Following this, the previously proposed Geiger-Nuttal law [23] of α radioactivity can be nicely explained despite the lack of details on the composition of an α particle or even the atomic nucleus. There is in fact a coincidence that the formation probability of the α cluster before its emission varies smoothly, particularly in contrast with the varying range of the penetration probability (more than 30 orders of magnitude). Consequently, the experimental α decay half-lives can be well reproduced within various theoretical models plus the constant assumption of an α preformation factor [24–28].

In turn, the α preformation factor (P_α) can be extracted from the experimental half-life and the calculated penetration probability [29–37] (or say the decay width). The abnormal behavior of P_α away from the expected smooth trend can then exhibit the special characteristic of exotic nuclei [38,39], such as the aforementioned shell effect [40–44] and the enhancement of proton-neutron correlation [15,45]. However, the extracted values of P_α are quite model-dependent because the penetration is addressed within a specific α-core interaction potential, which is constructed via different ways in different models. It seems that these conjectures or conclusions, based on the extraction of the α preformation factor, are therefore model dependent as well. Fortunately, the key point is a deviation of P_α from the relatively flat trend, leading to our new knowledge of the structural properties of nuclei away from the stability line. The latter P_α lines, on the basis of different α decay models, can actually shift together into a generally single one, as shown in our previous study to some extent [32]. Despite differences in the extracted P_α values [33,46–50], the overall conclusion drawn from the observed trends should remain consistent.

In this study, we propose a model-independent avenue to recognize the regular pattern of preformation probability P_α in heavy nuclei near the proton drip line. Specifically, we obtain the ratio of the calculated decay width of one α emitter to its lighter neighbor in one isotopic chain. In parallel, the ratio of experimental half-lives is correspondingly presented. If the α preformation probability varies smoothly, these two

*qyibin@njust.edu.cn

lines of ratios should be close with each other. It can be simply figured out that such a comparison is not related with the choice of α decay models in fact. Moreover, a slightly modified Woods-Saxon type potential is adopted by us to systematically describe the α-core structure recently. Given the same α-core two-body system, the same potential is applied here to calculate the decay width to make the investigation consistent. Another new ingredient, here, is that the decay width is obtained in view of the pure particle flow via the solution of the radial α-core Schrödinger equation. The details on the present approach can be found in the next section, in which the cluster formation model is also employed to perform a comparative study on the α preformation factor. In Sec. III, specific results and related discussions are presented, followed by a summary in the last section.

II. THEORETICAL FRAMEWORK

A. Extraction of α preformation factor from the experimental data

Once the α particle is formed at the nucleus surface, it combines with the residual daughter nucleus to create a two-body system, leading to a quasibound state, corresponding to a decay width. As for this α-core system, the radial wave function can be achieved by solving the relative motion Schrödinger equation between the α particle and residual nucleus, which is given by

$$\left(\frac{-\hbar^2}{2m}\nabla^2 + V(r)\right)u_{n\ell m} = Q_\alpha u_{n\ell m}. \tag{1}$$

Here, the total interaction potential $V(r)$ consists of the nuclear potential $V_N(r)$, the repulsive Coulomb potential $V_C(r)$, and the additional centrifugal potential,

$$V(r) = V_N(r) + V_C(r) + \frac{\hbar^2\ell(\ell+1)}{2\mu r^2}, \tag{2}$$

where μ is the reduced mass of the α-core system, ℓ is the angular momentum carried by the α particle, and r denotes the distance between the center of mass of the residual daughter nucleus and that of the α cluster. Actually, the angular momentum carried by α emitted is zero for ground state(g.s.) to g.s. α transitions of even-even nuclei here.

After the residual daughter nucleus is treated as an isotropic spheroid with homogeneous charges plus the point approximation of α particle, the repulsive Coulomb potential $V_C(r)$ can be obtained by

$$V_C(r) = \begin{cases} \frac{Z_d Z_\alpha e^2}{r}, & \mathrm{r} > \mathrm{R_C} \\ \frac{Z_d Z_\alpha e^2}{2R_C}\left[3 - \left(\frac{r}{R_C}\right)^2\right], & \mathrm{r} \leqslant \mathrm{R_C} \end{cases}, \tag{3}$$

where R_C is the Coulomb radius, Z_d and Z_α denotes the charge number of core and cluster of the system, respectively.

It is obvious that the selection of the nuclear potential $V_N(r)$ is a crucial step in determining $V(r)$, while the different theoretical models employ different interaction potentials [34,37,51–53]. Our previous study [54] utilized a Woods-Saxon type potential plus a high order term (i.e ., W.S.+W.S.^{3}) to investigate the cluster structure above the double magic nucleus,

$$V_N(r) = -V_0\left[1 + \lambda\exp\left(-\frac{r^2}{\sigma^2}\right)\right] \times \left\{\frac{b}{1+\exp[(r-R)/a]} + \frac{1-b}{\{1+\exp[(r-R)/3a]\}^3}\right\}, \tag{4}$$

where V_0, λ, σ, a, and b are fixed parameters. In order to ensure the consistency with previous research [54], the same nuclear potential $V_N(r)$ [i.e., Eq. (4)] is adopted here with its corresponding parameters to investigate the same two-body system. The determination of the separation radius R for each nucleus is obtained by adjusting the experimental decay energy Q_α values, where the special number of internal nodes is determined by the Wildermuth condition,

$$G = 2N + \ell = \sum_{i=1}^{4}(2n_i + \ell_i) = \sum_{i=1}^{4} g_i. \tag{5}$$

Here, N is the number of internal nodes, n_i and ℓ_i are the corresponding quantum numbers of the nucleons forming the α cluster in the shell model context. The globe quantum number is therefore chosen as $G = 22$ ($G = 20$) for nuclei with the neutron number $N > 126$ ($N \leqslant 126$), which is consistent with previous studies [55–57]. Following this schedule, one can find that the separation radius R shows a clear change when crossing the $N = 126$ shell closure, which is not consistent with the continuous behavior of experimental charge radii in this region [58]. To address this issue, the potential depth V_0 should be tuned up slightly above $N = 126$ to ensure the continuity of R around the closed-shell region.

A methodology of analyzing the quasibound state wave function in the pure particle emission state is utilized to evaluate the decay width through the determination of energy flux density at the remote region. In the case of pure particle emission, the quasibound state normalized wave function can be solved by matching the outgoing Coulomb wave function in the asymptotic zone, namely,

$$u_{n\ell m}(r) \backsimeq A(G_\ell(kr) + iF_\ell(kr)) \longrightarrow A\exp(ikx + \delta). \tag{6}$$

It is worthwhile to note that the wave function of real and imaginary parts both maintains a stable amplitude A in the asymptotic region. Two randomly adjacent points r_1 and r_2 are picked in the asymptotic region, and u_1 $(r_1) = 1$ $[u_2(r_1) = 1]$ and $u_1(r_2) = 1$ $[u_2(r_2) = -1]$ are taken as the corresponding wave functions, respectively. There are only two linearly independent solutions in the quasibound state wave function, $u_1(r_1)$ and $u_1(r_2)$ can then be derived by linearly superimposing the real and imaginary components of Eq. (6):

$$u_1 = \frac{\cos\theta}{\cos\theta + \sin\theta}\mathrm{Re}(u_{n\ell m}) + \frac{\sin\theta}{\cos\theta + \sin\theta}\mathrm{Im}(u_{n\ell m}),$$
$$u_2 = \frac{\sin\theta}{\cos\theta - \sin\theta}\mathrm{Re}(u_{n\ell m}) + \frac{\cos\theta}{\cos\theta - \sin\theta}\mathrm{Im}(u_{n\ell m}), \tag{7}$$

where θ is the phase difference between u_1 and $\mathrm{Re}(u_{n\ell m})$. With the process presented above, the amplitudes A_1 and A_2 in the asymptotic region can be obtained by

$$A_1 = \frac{A}{|\cos\theta + \sin\theta|},$$
$$A_2 = \frac{A}{|\cos\theta - \sin\theta|}, \tag{8}$$

where A_1 and A_2 are the amplitude of the wave functions u_1 and u_2, respectively. After A_1 and A_2 are calculated, the amplitude A of the pure outflow state wave function $u_{n\ell m}$ in the asymptotic region can be given by

$$\lim_{r\to\infty} |\Psi_{n\ell m}(r)|^2 = A^2 = \frac{2A_1^2A_2^2}{A_1^2 + A_2^2}. \tag{9}$$

In order to avoid the singularity in the calculation of A_1 and A_2, one needs to reselect the starting points in the asymptotic zone if the difference between A_1 and A_2 is very large. After the asymptotic behavior of the quasibound state wave function in the outflow state is obtained, the α decay width can be achieved by

$$\Gamma = \frac{\hbar^2 k}{\mu} A^2, \tag{10}$$

where the wave number $k = \sqrt{2\mu E}/\hbar$. As for the half-lives of α decay, one can obtain

$$T_{1/2} = \frac{\hbar \ln 2}{P_\alpha \Gamma}, \tag{11}$$

where P_α is the preformation factor. It is believed that P_α is quite difficult to be evaluated microscopically because of the complexity of both the nuclear potential and the nuclear many-body problem. In turn, the extracted P_α values, from the experimental half-life and calculated decay width based on the above equation, can tell us structural features of exotic α emitters. However, previous studies have proven that the Γ is sensitive to the choice of the α-core interaction potential, and it can span quite large orders of magnitude in different models. Hence the model-independent analysis on the α preformation factor, aiming at the rich knowledge of dynamical behavior derived by the nucleon-nucleon correlation, should be necessary. As mentioned before, one can avoid the discrepancies due to the model choice by considering the ratios of related quantities (i.e., $T_{1/2}$, Γ, and P_α) of adjacent nuclei in the isotopic chain. In detail, the ratio of P_α of neighboring nuclei, according to Eq. (11), can be assessed by

$$R_\alpha = \frac{P_{\alpha(n)}}{P_{\alpha(n+1)}} = \frac{T_{1/2(n+1)}/T_{1/2(n)}}{\Gamma_n/\Gamma_{n+1}}, \tag{12}$$

where n denotes one certain nucleus and $n+1$ denotes its isotopic neighbor with one more neutron.

B. α preformation factor with the cluster-formation model

To compare the present extracted P_α values plus the ratios with other results from a relatively direct method, the α preformation factor is also evaluated within the cluster-formation model (CFM). According to the CFM, the initial state wave function of the nuclear system Ψ can be described as a linear combination of possible clusterization states Ψ_i, namely,

$$\Psi = \sum_{i=1}^{N} a_i \Psi_i, \tag{13}$$

where a_i is the superposition coefficient of clusterization states Ψ_i. In parallel, the total Hamiltonian H can be written as the combination of all cluster Hamiltonians H_i,

$$H = \sum_{i=1}^{N} H_i. \tag{14}$$

Note that various clusterization states are degenerate for the total energy E of the system within the CFM framework. Additionally, the conditions of orthogonality and completeness are satisfied between these different clusterization states,

$$\sum_{i=1}^{N} |a_i|^2 = 1, \tag{15}$$
$$a_i = \int \Psi_i^* \Psi d\tau. \tag{16}$$

Following this, one can get the relation about the eigenenergy E of the total wave function,

$$E = \sum_{i=1}^{n} |a_i|^2 E = \sum_{i=1}^{n} E_{fi}, \tag{17}$$

where E_{fi} represents the formation energy of the clusterization state Ψ_i. According to the above process, the formation probability P_i of the clusterization state Ψ_i of the initial state wave function can be denoted as $P_i = |a_i|^2 = E_{fi}/E$. Obviously, the formation probability of a certain clusterization state can be determined by the ratio of its formation energy to the total energy of the system. Consequently, in the case of four-nucleon clusterization, i.e., α particle, the formation probability of α cluster can be given by

$$P_\alpha^{\mathrm{CFM}} = \frac{E_{f\alpha}}{E}, \tag{18}$$

where $E_{f\alpha}$ denotes the formation energy of the α cluster state and E is the total energy composed of $E_{f\alpha}$ and the interaction energy between the α cluster and the residual daughter nucleus. In principle, to determine the formation energy $E_{f\alpha}$ and the total energy E shown in Eq. (18), the overlap integral of the wave function between the initial state and the α-decaying state should be obtained by separating the complete Hamiltonian within the coordinate transformation and subsequently solving the time-dependent Schrödinger equation [41,49,59–61]. It is worthwhile to note that the main contribution to the α cluster formation probability stems from the nucleons at the surface of the parent nucleus [62–64]. As a consequence, the experimental data of the binding energy can be utilized to approximate the values of the previously indicated two energies leading to the preformation probability in the CFM. By carefully analyzing the nucleon-nucleon interactions of neutrons $(n-n)$ and protons $(p-p)$ as well as neutron-proton

$(n-p)$ correlations on the surface of the nucleus, explicit expressions of the formation energy and total energy have been given, namely [59],

$$E_{f\alpha} = 3B(A,Z) + B(A-4,Z-2) - 2B(A-1,Z-1) - 2B(A-1,Z), \quad (19)$$

$$E = S_\alpha(A,Z) = B(A,Z) - B(A-4,Z-2), \quad (20)$$

where S_α are α-cluster separation energies. To obtain a more concise link between the formation energy $E_{f\alpha}$ and the nucleon-nucleon interacting energy,i.e., separation energies, one can reformulate Eq. (19) to

$$E_{f\alpha} = E_{f\alpha} + B(A-4,Z-2) - B(A-4,Z-2) = [2S_p(A,Z) + 2S_n(A,Z)] - S_\alpha(A,Z), \quad (21)$$

where S_p (S_n) denotes the single-proton (neutron) separation energy of the parent nucleus, namely,

$$S_p(A,Z) = B(A,Z) - B(A-1,Z-1), \quad (22)$$

$$S_n(A,Z) = B(A,Z) - B(A-1,Z). \quad (23)$$

As mentioned in Ref. [49], Eqs. (19) and (20) can only effectively reproduce the preformation factors P_α for even-even nuclei. It will be unreasonable when extending to the formation energy $E_{f\alpha}$ of odd-odd and odd-A nuclei. At that time, based on the above equation (21), the reasonable relation of the formation energy for different types (even-even, odd-odd, odd-A) of nuclei was proposed [41,49]:

$$E_{f\alpha} = \begin{cases} 2S_p + 2S_n - S_\alpha & (\textbf{even}-\textbf{even}) \\ 2S_p + S_{2n} - S_\alpha & (\textbf{even}-\textbf{odd}) \\ S_{2p} + 2S_n - S_\alpha & (\textbf{odd}-\textbf{even}) \\ S_{2p} + S_{2n} - S_\alpha & (\textbf{odd}-\textbf{odd}) \end{cases}. \quad (24)$$

Here, the S_{2p} (S_{2n}) denotes the two-proton (neutron) separation energy as

$$S_{2p}(A,Z) = B(A,Z) - B(A-2,Z-2), \quad (25)$$

$$S_{2n}(A,Z) = B(A,Z) - B(A-2,Z). \quad (26)$$

In short, owing to the concisely refined equation, i.e., Eq. (18), proposed in the CFM scheme, a comparative relation to verify the consistency of the P_α between adjacent nuclei is simply given by

$$R_\alpha^{\mathrm{CFM}} = \frac{P_{\alpha(n)}}{P_{\alpha(n+1)}} = \frac{E_{f\alpha(n)}/E_n}{E_{f\alpha(n+1)}/E_{n+1}}. \quad (27)$$

III. CALCULATED RESULTS AND DISCUSSION

Based on the theoretical framework described above, we intend to investigate the pattern of α preformation factors in heavy α emitters with a focus on the g.s. to g.s α decays in even-even nuclei with $82 < Z < 92$ and $102 < N < 144$. Before showing the detailed results of the α preformation factor, the ratios (in logarithm scale) of experimental α decay widths deduced from the measured data [65] and the calculated ones for isotopic chains are presented in Fig. 1. As one can see, the

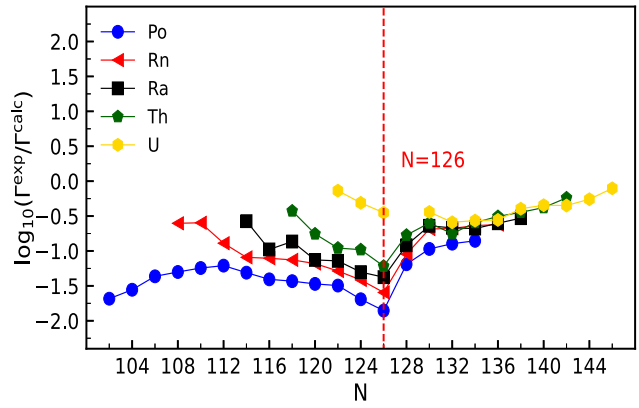

FIG. 1. The logarithm of ratios between the experimental α decay widths and the calculated ones for isotopic chains versus the neutron number N of α-decaying nuclei.

$\log_{10}(\Gamma^{\mathrm{exp}}/\Gamma^{\mathrm{calc}})$, corresponding to the α preformation factor, as implied by Eq. (11), clearly decreases in the vicinity of the $N = 126$ shell closure for each isotopic chain. This reconfirms the significant shell effect in the formation process of the α cluster, which is consistent with previous studies [46,66,67]. It is noted that the $\log_{10}(\Gamma^{\mathrm{exp}}/\Gamma^{\mathrm{calc}})$, as another form of P_α, generally maintains steady values when it comes to the off-shell region. The interesting point is that this quantity of the α emitter above $N = 126$ is obviously higher than that of nuclei with $N < 126$, which can be attributed to the strong pairing force among the neutrons and protons for the α particle formation [15]. Moreover, the abnormal behavior of uranium isotopes below $N = 126$ can be understood from the enhanced $n-p$ correlation with an increasing number of valence protons, as shown in the recent systematical analysis [15].

Figure 1 actually denotes that the extracted P_α values are in the reasonable order of 10^{-1} based on Eq. (11). In fact, the discrepancies of calculated α decay widths, from different models [51–53,68–73], can span several orders of magnitude, denoting large differences between various extracted preformation factors. For example, the evaluated P_α values from the present extraction and the CFM method are shown in parallel for Po and Ro isotopes in Fig. 2. As anticipated, the value of P_α is comparatively small in the vicinity of the $N = 126$ shell closure along the isotopic chain, no matter if the extraction or the CFM evaluation is concerned. For instance, ^{210}Po and ^{212}Rn hold the smallest P_α values among the polonium and radon isotopes, respectively.

Besides reconfirming the strong shell effect on the formation of the α cluster, this supports our previous points that the deviation away from the general trend is the key for demonstrating the structural properties from the α preformation probability. Based on the careful analysis in our previous study [32], it is found that the extracted preformation factors exhibit a similar variation trend for each isotopic chain, whichever model is employed in the calculation of the α decay width. Of course, the previous results [32] and the present discussion on the preformation probabilities from Fig. 2 are quite intuitive rather than directive presentation. It is therefore, as

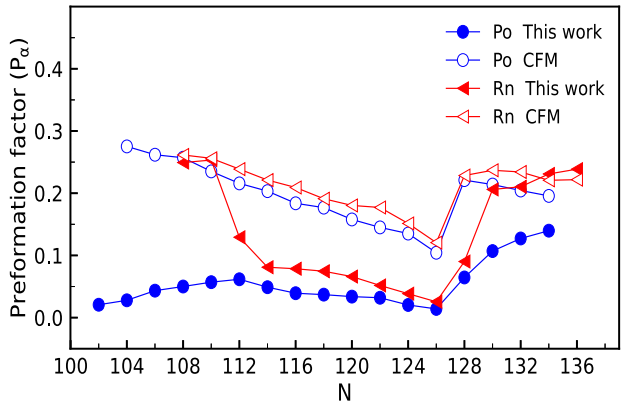

FIG. 2. The comparison of the α preformation factor in the present extraction (solid symbols) with that within the CFM (hollow symbols) versus the neutron number of parent nuclei.

mentioned before, necessary to perform a model-independent way to recognize the P_α pattern, serving as a probe into the $n-p$ interaction [15], shell evolution [44], symmetry energy [74], and other structural phenomenon.

Before paying attention to the extracted or evaluated P_α values directly, let us mention the comparison of the ratio of the half-life between two adjacent nuclei with that of calculated decay width (Γ_n/Γ_{n+1}) in isotopes, as shown in Fig. 3. This parallel comparison, inspired by Eq. (12), can unravel the varying trend of the α preformation factor. Indeed, the order of magnitude, for these two quantities $\log_{10}(T_{1/2(n+1)}/T_{1/2(n)})$ and $\log_{10}(\Gamma_n/\Gamma_{n+1})$, is identical as shown in Fig. 3, which has not been dependent on the choice of the α-core interaction potential. It will be interesting to see the corresponding ratios

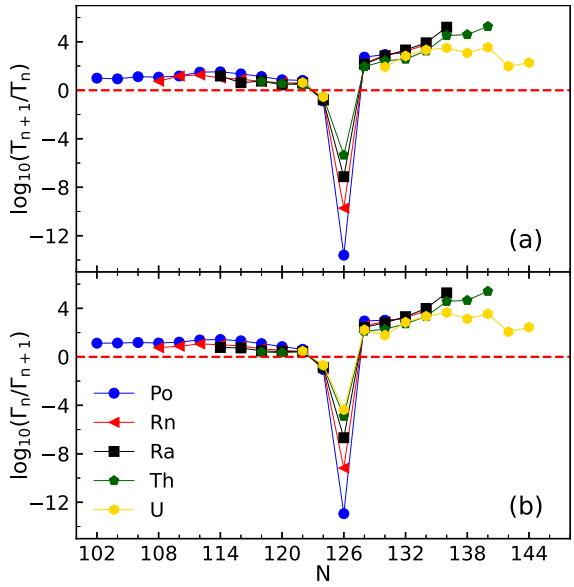

FIG. 3. Ratios of the experimental half-life (a) and the calculated decay width (b) versus the neutron number N of α emitters. Here, the subscripts n and $n+1$ denote two adjacent nuclei in the even-even isotopic chain.

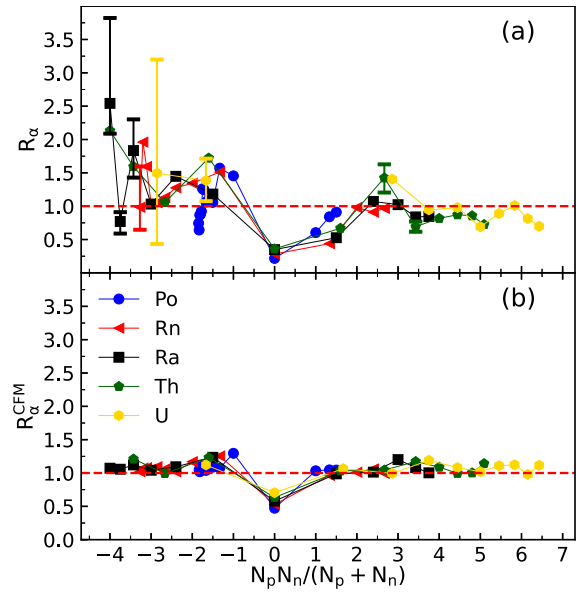

FIG. 4. Comparison of the preformation factor ratios extracted from the experimental data (a) with those from the CFM evaluation (b). The ratios are plotted versus the standard Casten parameter $[N_pN_n/(N_p+N_n)]$ for isotopic chains.

of decay widths calculated from other models. The close behaviors of these two ratios of experimental half-life and calculated decay width substantiate the smooth and steady pattern of preformation factors again. Moreover, the values of $\log_{10}(T_{1/2(n+1)}/T_{1/2(n)})$ and $\log_{10}(\Gamma_n/\Gamma_{n+1})$ on the right part above the $N=126$ shell are generally larger than those on the left region, which is a manifestation of the different changing rates of both half-lives and α-decay widths crossing the $N=126$ shell closure. This may be explained by the aforementioned strong neutron-neutron pairing ($n-n$) interaction there. Simply, increasing the valence neutron would make the α emission harder, resulting in the reduction of α decay energy (very sensitive to the calculated decay width and half-life). As a result, the α decay half-life of heavier isotopes with $N>126$ is comparatively longer plus an increasing rate, as shown in the right panel of Fig. 3. The shell effect is expected to interplay with the pairing correlation for the preformation of the α cluster before its penetration [12], as evidenced in recent experiments as well [75,76]. In Fig. 4, the ratio of P_α in one isotopic chain, defined as R_α previously, is plotted versus the quantity $N_pN_n/(N_p+N_n)$. In this context, the N_p (N_n) represents the valence proton (neutron) number with respect to the nearest shell closure, i.e., $Z=82$ and $N=126$ here, which was earlier proposed by Casten [77] in the pursuit of the relations of $n-p$ pairing correlations with nuclear structure information. As shown in the top panel of Fig. 4, the ratio value R_α varies quite smoothly and approaches the unity line in the right region across the $N=126$ shell closure. As compared, there is is relatively obvious fluctuation for the R_α value at the left side from the $N_pN_n=0$ point, which could be explained as follows to some extent. On one hand, the extracted uncertainties can be further reduced with the improving accuracy of the experimental α decay data

especially in the uranium and radon isotopes near the proton drip line. On the other hand, with the introduction of more valence neutrons (or holes) in the α formation process, the situation would be more complicated leading to the fluctuant pattern of the α preformation factor there. Further, the R_α varies in general smoothly especially for nuclei with $N > 126$ in the $n-p$ related context, namely N_pN_n, which implies the slight effect from the $n-p$ interaction in the α formation. This is also consistent with the recent conjecture on the basis of the experimental α decay systematics around ^{208}Pb. Meanwhile, those α-decaying nuclei above ^{100}Sn are in different circumstances due to the expectedly large $n-p$ correlation within a closer Fermi surface of protons and neutrons. In this nuclear symmetry region ($N \sim Z$), the α preformation probability should be therefore larger, which has been demonstrated via the relative α-reduced width [8,78]. As for the CFM evaluation, the $R_\alpha^{\rm CFM}$ value holds quite steadily away from the closed shell, implying the smooth P_α value. This is generally consistent with the above extracted result [Fig. 4(a)], sustaining the previous knowledge of the P_α behavior in a model-independent way. Moreover, the logarithm of the preformation probability is linearly related with the square root of the decay energy for isotopes [79,80]. The α decay energy of emitters, away from the shell, is also linear with the neutron number for isotopic chains, as opposed to the valence correlation scheme or the systematics analysis [81,82]. Keeping these two facts in mind, it can be easily concluded that the ratio of P_α between neighboring α emitters would maintain in a smooth pattern. Yet it is worth noting that the CFM is derived from the assumption of clusterization states, neglecting the detailed nucleon-nucleon or cluster-cluster correlation. A further investigation deserves the more accurate description of the α preformation factor, helping the experimental design for the synthesis of superheavy α-decaying nuclei.

IV. SUMMARY

In summary, our recently proposed technique, focusing on the asymptotic behavior of the radial wave function of the α-core relative motion, is applied to systematically calculate the α decay width of heavy isotopes with $Z > 82$. During this process, the crucial α-core potential is directly chosen from previous studies of α cluster structure, to ensure the consistency of investigation on the same binary system. The α preformation probability is then extracted by the obtained decay width and the corresponding measured half-life for isotopic chains. After the detailed analysis of these three related quantities, namely $T_{1/2}$, Γ, and P_α, via the ratio of them between adjacent α emitters, the generally smooth pattern of the preformation factor in the off-shell region is revealed in a model-independent way not to mention the strong effect of the $N = 126$ shell. Meanwhile, the neutron-proton pairing is supposed to play a key role in the slightly different P_α behavior at two sides of the $N = 126$ shell closure, implying the interplay between the shell effect and pairing in the formation of the α cluster before its emission. The evaluated preformation factors from the cluster formation model are also given for comparison, supporting the conjecture in this study. It is hoped that the present strategy can be applied to other α decay models, further enriching the knowledge of clustering in heavy and superheavy nuclei.

ACKNOWLEDGMENTS

This work is supported by the National Natural Science Foundation of China (Grants No. 12075121, No. 12035011, and No. 11975167), by the Natural Science Foundation of Jiangsu Province (Grant No. BK20190067), by the Fundamental Research Funds for the Central Universities (Grant No. 30922010312), and by the National Key R&D Program of China (Grant No. 2018YFA0404403).

[1] Y. Oganessian and V. Utyonkov, Nucl. Phys. A **944**, 62 (2015).
[2] G. Münzenberg, Nucl. Phys. A **944**, 5 (2015).
[3] K. Morita, Nucl. Phys. A **944**, 30 (2015).
[4] S. Hofmann, J. Phys. G: Nucl. Part. Phys. **42**, 114001 (2015).
[5] S. N. Liddick, R. Grzywacz, C. Mazzocchi, R. D. Page, K. P. Rykaczewski, J. C. Batchelder, C. R. Bingham, I. G. Darby, G. Drafta, C. Goodin, C. J. Gross, J. H. Hamilton, A. A. Hecht, J. K. Hwang, S. Ilyushkin, D. T. Joss, A. Korgul, W. Królas, K. Lagergren, K. Li *et al.*, Phys. Rev. Lett. **97**, 082501 (2006).
[6] I. G. Darby, R. K. Grzywacz, J. C. Batchelder, C. R. Bingham, L. Cartegni, C. J. Gross, M. Hjorth-Jensen, D. T. Joss, S. N. Liddick, W. Nazarewicz, S. Padgett, R. D. Page, T. Papenbrock, M. M. Rajabali, J. Rotureau, and K. P. Rykaczewski, Phys. Rev. Lett. **105**, 162502 (2010).
[7] A. N. Andreyev, M. Huyse, P. Van Duppen, C. Qi, R. J. Liotta, S. Antalic, D. Ackermann, S. Franchoo, F. P. Heßberger, S. Hofmann, I. Kojouharov, B. Kindler, P. Kuusiniemi, S. R. Lesher, B. Lommel, R. Mann, K. Nishio, R. D. Page, B. Streicher, S. Šáro *et al.*, Phys. Rev. Lett. **110**, 242502 (2013).
[8] K. Auranen, D. Seweryniak, M. Albers, A. D. Ayangeakaa, S. Bottoni, M. P. Carpenter, C. J. Chiara, P. Copp, H. M. David, D. T. Doherty, J. Harker, C. R. Hoffman, R. V. F. Janssens, T. L. Khoo, S. A. Kuvin, T. Lauritsen, G. Lotay, A. M. Rogers, J. Sethi, C. Scholey *et al.*, Phys. Rev. Lett. **121**, 182501 (2018).
[9] K. P. Santhosh and C. Nithya, Phys. Rev. C **97**, 064616 (2018).
[10] A. Dumitrescu and D. Delion, At. Data Nucl. Data Tables **145**, 101501 (2022).
[11] Z. Y. Zhang, Z. G. Gan, H. B. Yang, L. Ma, M. H. Huang, C. L. Yang, M. M. Zhang, Y. L. Tian, Y. S. Wang, M. D. Sun, H. Y. Lu, W. Q. Zhang, H. B. Zhou, X. Wang, C. G. Wu, L. M. Duan, W. X. Huang, Z. Liu, Z. Z. Ren, S. G. Zhou *et al.*, Phys. Rev. Lett. **122**, 192503 (2019).
[12] Y. Lei, S. Pittel, N. Sandulescu, A. Poves, B. Thakur, and Y. M. Zhao, Phys. Rev. C **84**, 044318 (2011).
[13] R. I. Betan and W. Nazarewicz, Phys. Rev. C **86**, 034338 (2012).
[14] V. V. Baran and D. S. Delion, Phys. Rev. C **94**, 034319 (2016).
[15] Z. Y. Zhang, H. B. Yang, M. H. Huang, Z. G. Gan, C. X. Yuan, C. Qi, A. N. Andreyev, M. L. Liu, L. Ma, M. M. Zhang, Y. L. Tian, Y. S. Wang, J. G. Wang, C. L. Yang, G. S. Li, Y. H. Qiang, W. Q. Yang, R. F. Chen, H. B. Zhang, Z. W. Lu *et al.*, Phys. Rev. Lett. **126**, 152502 (2021).

[16] G. Casini, S. Piantelli, P. R. Maurenzig, A. Olmi, L. Bardelli, S. Barlini, M. Benelli, M. Bini, M. Calviani, P. Marini, A. Mangiarotti, G. Pasquali, G. Poggi, A. A. Stefanini, M. Bruno, L. Morelli, V. L. Kravchuk, F. Amorini, L. Auditore, G. Cardella *et al.*, Phys. Rev. C **86**, 011602(R) (2012).
[17] S. Sasabe, T. Matsumoto, S. Tagami, N. Furutachi, K. Minomo, Y. R. Shimizu, and M. Yahiro, Phys. Rev. C **88**, 037602 (2013).
[18] G. J. Fu, Y. Y. Cheng, H. Jiang, Y. M. Zhao, and A. Arima, Phys. Rev. C **94**, 024312 (2016).
[19] Y. Urata, K. Hagino, and H. Sagawa, Phys. Rev. C **96**, 064311 (2017).
[20] R. An, X. Jiang, L.-G. Cao, and F.-S. Zhang, Phys. Rev. C **105**, 014325 (2022).
[21] G. Gamow, Z. Phys. **51**, 204 (1928).
[22] R. W. Gurney and E. U. Condon, Nature (London) **122**, 439 (1928).
[23] H. Geiger and J. M. Nuttall, Philos. Mag. **22**, 613 (1911).
[24] B. Buck, A. C. Merchant, and S. M. Perez, Phys. Rev. C **51**, 559 (1995).
[25] D. S. Delion, A. Sandulescu, and W. Greiner, Phys. Rev. C **69**, 044318 (2004).
[26] C. Xu and Z. Ren, Nucl. Phys. A **760**, 303 (2005).
[27] C. Xu and Z. Ren, Phys. Rev. C **74**, 014304 (2006).
[28] Y. Z. Wang, S. J. Wang, Z. Y. Hou, and J. Z. Gu, Phys. Rev. C **92**, 064301 (2015).
[29] H. F. Zhang and G. Royer, Phys. Rev. C **77**, 054318 (2008).
[30] H. F. Zhang, G. Royer, Y. J. Wang, J. M. Dong, W. Zuo, and J. Q. Li, Phys. Rev. C **80**, 057301 (2009).
[31] Y. Qian and Z. Ren, Nucl. Phys. A **852**, 82 (2011).
[32] Y. Qian and Z. Ren, Sci. China Phys. Mech. Astron. **56**, 1520 (2013).
[33] Y. Z. Wang, J. Z. Gu, and Z. Y. Hou, Phys. Rev. C **89**, 047301 (2014).
[34] D. Ni and Z. Ren, Phys. Rev. C **92**, 054322 (2015).
[35] M. Ismail, A. Adel, and M. M. Botros, Phys. Rev. C **93**, 054618 (2016).
[36] P. Mohr, Phys. Rev. C **95**, 011302(R) (2017).
[37] X. D. Sun, J. G. Deng, D. Xiang, P. Guo, and X. H. Li, Phys. Rev. C **95**, 044303 (2017).
[38] C. Xu and Z. Ren, Phys. Rev. C **76**, 027303 (2007).
[39] G. Sawhney, M. K. Sharma, and R. K. Gupta, Phys. Rev. C **83**, 064610 (2011).
[40] M. Ismail, A. Y. Ellithi, M. M. Botros, and A. Adel, Phys. Rev. C **81**, 024602 (2010).
[41] D. Deng and Z. Ren, Phys. Rev. C **93**, 044326 (2016).
[42] X.-D. Sun, P. Guo, and X.-H. Li, Phys. Rev. C **94**, 024338 (2016).
[43] J. Zhang and H. F. Zhang, Phys. Rev. C **102**, 044308 (2020).
[44] C. He and J.-Y. Guo, Phys. Rev. C **106**, 064310 (2022).
[45] R. M. Clark, A. O. Macchiavelli, H. L. Crawford, P. Fallon, D. Rudolph, A. Såmark-Roth, C. M. Campbell, M. Cromaz, C. Morse, and C. Santamaria, Phys. Rev. C **101**, 034313 (2020).
[46] P. Mohr, Phys. Rev. C **73**, 031301(R) (2006).
[47] G. L. Zhang, X. Y. Le, and H. Q. Zhang, Phys. Rev. C **80**, 064325 (2009).
[48] K. P. Santhosh and T. A. Jose, Phys. Rev. C **99**, 064604 (2019).
[49] D. Deng, Z. Ren, D. Ni, and Y. Qian, J. Phys. G: Nucl. Part. Phys. **42**, 075106 (2015).
[50] J.-G. Deng and H.-F. Zhang, Phys. Rev. C **102**, 044314 (2020).
[51] S. A. Gurvitz and G. Kalbermann, Phys. Rev. Lett. **59**, 262 (1987).
[52] S. Peltonen, D. S. Delion, and J. Suhonen, Phys. Rev. C **78**, 034608 (2008).
[53] N. G. Kelkar and M. Nowakowski, Phys. Rev. C **89**, 014602 (2014).
[54] J. Jia, Y. Qian, and Z. Ren, Phys. Rev. C **104**, L031301 (2021).
[55] B. Buck, A. C. Merchant, and S. M. Perez, Phys. Rev. C **45**, 2247 (1992).
[56] C. Xu and Z. Ren, Phys. Rev. C **69**, 024614 (2004).
[57] D. Ni and Z. Ren, J. Phys. G: Nucl. Part. Phys. **37**, 035104 (2010).
[58] I. Angeli and K. Marinova, At. Data Nucl. Data Tables **99**, 69 (2013).
[59] S. M. S. Ahmed, R. Yahaya, S. Radiman, and M. S. Yasir, J. Phys. G: Nucl. Part. Phys. **40**, 065105 (2013).
[60] S. M. S. Ahmed, R. Yahaya, S. Radiman, M. S. Yasir, H. A. Kassim, and M. U. Khandaker, Eur. Phys. J. A **51**, 13 (2015).
[61] N. Wan and J. Fan, Phys. Rev. C **104**, 064320 (2021).
[62] G. Röpke, A. Schnell, P. Schuck, and P. Nozières, Phys. Rev. Lett. **80**, 3177 (1998).
[63] T. Sogo, G. Röpke, and P. Schuck, Phys. Rev. C **81**, 064310 (2010).
[64] G. Röpke, P. Schuck, Y. Funaki, H. Horiuchi, Z. Ren, A. Tohsaki, C. Xu, T. Yamada, and B. Zhou, Phys. Rev. C **90**, 034304 (2014).
[65] https://www.nndc.bnl.gov/.
[66] K. P. Santhosh, T. A. Jose, and N. K. Deepak, Phys. Rev. C **103**, 064612 (2021).
[67] D. S. Delion and A. Dumitrescu, Eur. Phys. J. A **59**, 210 (2023).
[68] R. Blendowske and H. Walliser, Phys. Rev. Lett. **61**, 1930 (1988).
[69] S. Åberg, P. B. Semmes, and W. Nazarewicz, Phys. Rev. C **56**, 1762 (1997).
[70] E. Maglione, L. S. Ferreira, and R. J. Liotta, Phys. Rev. Lett. **81**, 538 (1998).
[71] S. A. Gurvitz, P. B. Semmes, W. Nazarewicz, and T. Vertse, Phys. Rev. A **69**, 042705 (2004).
[72] H. Zhang, W. Zuo, J. Li, and G. Royer, Phys. Rev. C **74**, 017304 (2006).
[73] W. M. Seif, M. Shalaby, and M. F. Alrakshy, Phys. Rev. C **84**, 064608 (2011).
[74] J. Liu, Z. Ren, C. Xu, and R. Xu, Phys. Rev. C **88**, 024324 (2013).
[75] J. Khuyagbaatar, A. Yakushev, C. E. Düllmann, D. Ackermann, L.-L. Andersson, M. Block, H. Brand, D. M. Cox, J. Even, U. Forsberg, P. Golubev, W. Hartmann, R.-D. Herzberg, F. P. Heßberger, J. Hoffmann, A. Hübner, E. Jäger, J. Jeppsson, B. Kindler, J. V. Kratz *et al.*, Phys. Rev. Lett. **115**, 242502 (2015).
[76] L. Ma, Z. Y. Zhang, Z. G. Gan, X. H. Zhou, H. B. Yang, M. H. Huang, C. L. Yang, M. M. Zhang, Y. L. Tian, Y. S. Wang, H. B. Zhou, X. T. He, Y. C. Mao, W. Hua, L. M. Duan, W. X. Huang, Z. Liu, X. X. Xu, Z. Z. Ren, S. G. Zhou *et al.*, Phys. Rev. Lett. **125**, 032502 (2020).
[77] R. Casten, Nucl. Phys. A **443**, 1 (1985).
[78] D. Deng, Z. Ren, and N. Wang, Eur. Phys. J. A **59**, 226 (2023).
[79] Y. Qian and Z. Ren, Chin. Phys. C **45**, 021002 (2021).
[80] J.-G. Deng and H.-F. Zhang, Phys. Lett. B **816**, 136247 (2021).
[81] C. Xu and Z. Ren, Phys. Rev. C **74**, 037302 (2006).
[82] J. Jia, Y. Qian, and Z. Ren, Phys. Rev. C **103**, 024314 (2021).